

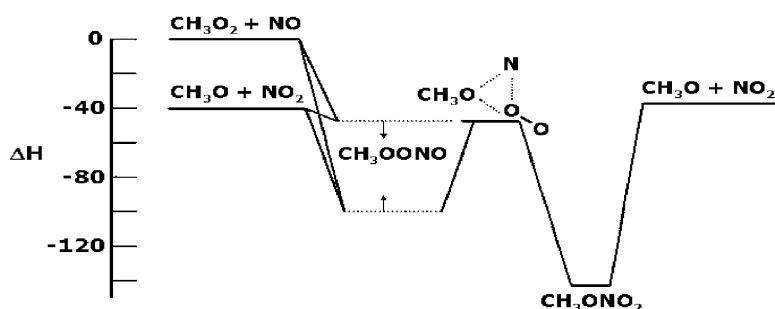
Article

Proton Affinity of Methyl Nitrite and Methyl Peroxynitrite: Implications for Measuring Branching Ratios of Alkyl Nitrates and Nitrites

Rose M. Ravelo, and Joseph S. Francisco

J. Am. Chem. Soc., **2008**, 130 (33), 11234-11239 • DOI: 10.1021/ja8045662 • Publication Date (Web): 29 July 2008

Downloaded from <http://pubs.acs.org> on February 8, 2009



More About This Article

Additional resources and features associated with this article are available within the HTML version:

- Supporting Information
- Access to high resolution figures
- Links to articles and content related to this article
- Copyright permission to reproduce figures and/or text from this article

[View the Full Text HTML](#)

Proton Affinity of Methyl Nitrite and Methyl Peroxynitrite: Implications for Measuring Branching Ratios of Alkyl Nitrates and Nitrites

Rose M. Ravelo and Joseph S. Francisco*

Department of Chemistry and Department of Earth and Atmospheric Science, Purdue University, West Lafayette, Indiana 47906

Received June 16, 2008; E-mail: francisc@purdue.edu

Abstract: Geometry optimizations for methyl nitrite and methyl peroxynitrite, along with various protonated isomers for each, have been investigated using ab initio and density functional methods. The lowest energy structure for protonated methyl nitrite is a complex between CH₃OH and NO⁺. For methyl peroxynitrite, the lowest energy protonated structure is a complex between CH₃OOH and NO⁺. Their respective proton affinities are estimated to be 195.2 and 195.8 kcal/mol at the QCISD(T)/6-311++G(3df,3pd) level of theory. The results, compared with past studies, suggest an alternative method for directly measuring branching ratios for production of alkyl nitrates and nitrites.

I. Introduction

Methyl nitrate (CH₃ONO₂) is in a class of compounds known as alkyl nitrates (RONO₂).¹ They account for 80% of the reactive nitrogen found in the troposphere.² Previous observations of alkyl nitrates (methyl, ethyl, and propyl) in remote marine atmospheres suggests that the oceans are a source of alkyl nitrates to the troposphere, accounting for 20–30% of the reactive nitrogen.^{3–9} It has been suggested that alkyl nitrates may form in seawater by a photochemical mechanism comparable to the one occurring in the polluted atmosphere.² Oceanic alkyl nitrates have not been well-studied and their origins are not well-known. Biomass burning is another potential source for alkyl nitrates.¹⁰

There are several pathways for the formation of methyl nitrate, including the reaction of RO with NO₂. This reaction becomes unimportant when RO undergoes reactions with other competing reactions that are much faster; however, this reaction does occur

in the troposphere at high concentrations of NO₂. Methyl nitrates are primarily found in NO_x-rich regions. Its atmospheric lifetime has been found to be a week or more at the Earth's surface and several days at higher altitudes. Its lifetime is long enough for methyl nitrate to play a role in the long-range transport of NO_x. The mechanism for the formation of alkyl nitrates could help shed some light into how they are produced in the atmosphere.^{11,12} The reaction of alkylperoxy radicals with nitric oxide to produce organic nitrates in the gas phase was first reported in 1976 by Darnall et al.:¹³



The major channel for the RO₂ + NO reaction is reaction 1. This propagates the radical chain leading to photochemical smog formation from the oxidation of NO to NO₂, ending in a net ozone production from the photolysis of NO₂. The second reaction path, reaction 2, terminates the radical chain through alkyl nitrate formation,¹⁴ creating a sink for NO_x. This becomes significant in NO-rich regions. Alkyl nitrate formation via reaction 2 becomes important as the size of the alkane or R-group increases.

The discovery of reaction 2 has been the topic of much discussion.^{15,16} It is widely accepted that both reactions 1 and 2 share a common intermediate, a peroxy nitrite (ROONO), whose decomposition governs the branching between radical

- (1) Finlayson-Pitts, B. J.; Pitts, J. N. *Chemistry of the Upper and Lower Atmosphere: Theory, Experiments and Applications*, 1st ed.; Academic Press: New York, 2000.
- (2) Dahl, E. E.; Saltzman, E. S.; deBruyn, W. J. *Geophys. Res. Lett.* **2003**, *30*, 1271.
- (3) Ellison, G. B.; Herbert, J. M.; McCoy, A. B.; Stanton, J. F.; Szalay, P. G. *J. Phys. Chem. A* **2004**, *108*, 7639.
- (4) Atlas, E.; Pollock, W.; Greenberg, J.; Heidt, L. J. *Geophys. Res.* **1993**, *98*, 16933.
- (5) Blake, N. J.; Blake, D. R.; Wingenter, O. W.; Sive, B. C.; Kang, C. H.; Thornton, D. C.; Bandy, A. R.; Atlas, E.; Flocke, F.; Harris, J. M.; Rowland, F. S. *J. Geophys. Res.* **1999**, *104*, 21803.
- (6) Atlas, E. *Nature* **1988**, *331*, 426.
- (7) Roberts, J. M.; Parrish, D. D.; Norton, R. B.; Bertman, S. B.; Holloway, J. S.; Trainer, M.; Fehsenfeld, F. C.; Carroll, M. A.; Albercook, G. M.; Wang, T.; Forbes, G. *J. Geophys. Res., [Atmos.]* **1996**, *101*, 28947.
- (8) Ridley, B. A.; Atlas, E. L.; Walega, J. G.; Kok, G.L.; Staffelbach, T.A.; Greenberg, J.P.; Grahek, F.E.; Hess, P. G.; Montzka, D. D. *J. Geophys. Res., [Atmos.]* **1997**, *102*, 18935.
- (9) Ballschmiter, K. *Science* **2002**, *297*, 1127.
- (10) Simpson, I. J.; Meinardi, S.; Blake, D. R.; Blake, N. J.; Rowland, F. S.; Atlas, E.; Flocke, F. *Geophys. Res. Lett.* **2002**, *29*, 2168.

- (11) Atkinson, R. *Atmos. Environ.* **2000**, *34*, 2063.
- (12) Atkinson, R. *J. Phys. Chem. Ref. Data* **1997**, *26*, 215.
- (13) Darnall, K. R.; Carter, W. P. L.; Winer, A. M.; Lloyd, A. C.; Pitts, J. N. *J. Phys. Chem.* **1976**, *80*, 1948.
- (14) Lightfoot, P. D.; Cox, R. A.; Crowley, J. N.; Destrian, M.; Hayman, G. D.; Jenkin, M. E.; Moortgat, G. K.; Zabel, F. *Atmos. Environ.* **1992**, *26A*, 1805.
- (15) Benson, S. W. *Thermochemical Kinetics*, 2nd ed.; Wiley: New York, 1976.
- (16) O'Brien, J. M.; Czuba, E.; D, R.; Francisco, J. S.; Shepson, P. B. *J. Phys. Chem. A* **1998**, *102*, 8903.

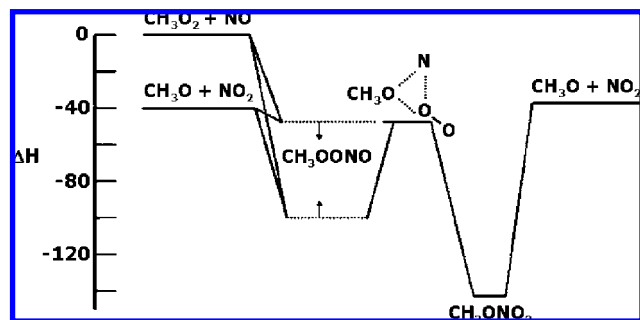


Figure 1. Energy diagram for the formation of alkyl nitrates and alkyl nitrites from the RO + NO₂ and RO₂ + NO reaction.

and nitrate.¹⁷ Figure 1 depicts an energy diagram that shows the mechanism of ROONO formation that isomerizes to form RONO₂. What is not as widely recognized is that the ROONO intermediate has two distinct conformers with separate chemical behaviors and fates.^{3,17,18} One conformer forms only to the radical products, and the other can form both radicals and nitrates. In terms of the variation of nitrate yields among different classes of peroxy radicals (primary, secondary, and tertiary alkyl-peroxy; B-hydroxy-peroxy radicals), Zhang and others^{19–23} note that this propensity may be governed by the initial branching between the ROONO conformers. In terms of the nitrate yields, Atkinson et al.,^{24–26} have observed a temperature dependence, (decreasing in yield with increasing temperature), as well as an observed pressure dependence (decreasing in yield with decreasing pressure), indicative of the collisional stabilization of these short-lived ROONO intermediates and their subsequent decomposition. Cassanelli et al.²⁷ also reported temperature-dependent alkyl nitrate yields at a fixed total pressure.

Significant reaction yields by numerous analytical methods^{14,24–35} have been measured that support nitrate formation

via reaction 2. To date, the only pressure-dependent organic nitrate yield data have been reported by Atkinson et al.,^{24,25} for alkyl nitrate formation from OH radical-initiated reactions using temperatures that range between 280–340 K and pressures between 55 and 740 Torr.²⁶ Arey et al.³⁶ found that the yield of alkyl nitrates increases with the carbon number of the *n*-alkane, (from <0.014 for ethane to ~0.23 for *n*-octane). These yields approach a limit of ~35% for large radicals, >C₉. Theoretical studies show that organic nitrates begin to form as the size of the alkyl group increases.³⁷ There are experimentally measured nitrate yield data for 22 secondary alkyl peroxy radicals formed either from NO_x–air photooxidations or from alkanes and alkenes.¹¹ Data are still needed on organic nitrates formation from volatile organic compounds (VOCs) observed in ambient air.^{38,39} However, for a given alkyl radical, the alkyl nitrate yield increases with increasing pressure and decreasing temperature. At a given temperature and pressure, the alkyl nitrate yields increase with increasing carbon number, at least for secondary RO₂ radicals.^{39,40} The recent data of Cassanelli et al.²⁷ show that the branching ratio increases along the series: secondary ~ tertiary > primary.

In terms of the mechanism, there is no clear understanding of why alkyl nitrate yields increase with increasing length of the R-group. The branching ratio, $k_2/(k_1 + k_2)$, sets the relative importance of chain propagation and termination and is dependent on the identity of R. Understanding the branching ratio is crucial for modeling of the tropospheric HO_x cycle, as nitrate formation is a radical-termination step, that leads to tropospheric ozone production.⁴¹ Because of the wide range of reactive atmospheric alkenes and alkanes that exist and the experimental difficulty in measuring the yields of relatively polar and adsorptive species, there is very little published data regarding organic nitrate yields for reactions of radicals with NO. It is desirable to have a firm understanding of the structural features that influence the branching ratio so that a predictive capability can be developed.⁴²

Calculations done by Lesar et al.⁴³ on the reaction of CH₃O₂ + NO suggest that the production of methyl nitrate occurs through the *trans*-peroxy nitrite isomerization channel if stabilization under suitable temperature and pressure conditions is possible. The calculations describe how one conformer proceeds directly to the radical products while the other proceeds to both nitrates and radical products, providing a mechanism that can explain the detection of trace quantities of methyl nitrate in the atmosphere. The measurements of Elrod et al.^{32,33} on the reaction of C₂H₅O₂ + NO and C₃H₇O₂ + NO show that the rate constants increase with decreasing temperature. This temperature dependence of the overall rate constants for these reactions agrees with the current recommendation for atmospheric modeling. Percival et al.^{34,35} studied the CH₃O₂ + NO and the C₂H₅O₂ + NO reactions and found that the branching ratio, $k_2/(k_1 + k_2)$

- (17) Zhang, J.; Dransfield, T.; Donahue, N. M. *J. Phys. Chem. A* **2004**, *108*, 9082.
 (18) Burkholder, J. B.; Hammer, P. D.; Howard, C. J. *J. Phys. Chem.* **1987**, *91*, 2136.
 (19) Carter, W. P. L.; Atkinson, R. *J. Atmos. Chem.* **1989**, *8*, 165.
 (20) Chen, X.; Hulbert, D.; Shepson, P. B. *J. Geophys. Res.* **1998**, *103*, 25563.
 (21) Sprengnether, M.; Demerjian, K. L.; Donahue, N. M.; Anderson, J. G. *J. Geophys. Res.* **2002**, *107*, 8-1–8-13.
 (22) Chuong, B.; Stevens, P. S. *J. Geophys. Res.* **2002**, *107*, 2-1–2-12.
 (23) Zhang, D.; Lei, W.; Zhang, R. *Chem. Phys. Lett.* **2002**, *358*, 171.
 (24) Atkinson, R.; Carter, W. P. L.; Winer, A. M. *J. Phys. Chem.* **1983**, *87*, 2012.
 (25) Atkinson, R.; Aschmann, S. M.; Winer, A. M. *J. Atmos. Chem.* **1987**, *5*, 91.
 (26) Aschmann, S. M.; Long, W. D.; Atkinson, R. *J. Phys. Chem. A* **2006**, *110*, 6617.
 (27) Cassanelli, P.; Fox, D. J.; Cox, R. A. *Phys. Chem. Chem. Phys.* **2007**, *9*, 4332.
 (28) Harris, S. J.; Kerr, J. A. *Int. J. Chem. Kinet.* **1989**, *21*, 207–218.
 (29) Roberts, J. M. *Atmos. Environ.* **1990**, *24A*, 243.
 (30) Wallington, T. J.; Nielsen, O. J.; Sehested, J. Reactions of Organic Peroxy Radicals in the Gas Phase. In *Peroxy Radicals*; Alfassi, Z. B., Ed.; John Wiley & Sons: Chichester, UK, 1997; pp 113–72.
 (31) Orlando, J. J.; Iraci, L. T.; Tyndall, G. S. *J. Phys. Chem. A* **2000**, *104*, 5072.
 (32) Ranschaert, D. L.; Schneider, N. J.; Elrod, M. J. *J. Phys. Chem. A* **2000**, *104*, 5758.
 (33) Chow, J. M.; Miller, A. M.; Elrod, M. J. *J. Phys. Chem. A* **2003**, *107*, 3040.
 (34) Bacak, A.; Bardwell, M. W.; Raventos, M. T.; Percival, C. J.; Sanchez-Reyna, G.; Shallcross, D. E. *J. Phys. Chem. A* **2004**, *108*, 10681.
 (35) Bardwell, M. W.; Bacak, A.; Raventos, M. T.; Percival, C. J.; Sanchez-Reyna, G. *Int. J. Chem. Kinet.* **2005**, *37*, 253.

- (36) Arey, J.; Aschmann, S. M.; Kwok, E. S. C.; Atkinson, R. *J. Phys. Chem. A* **2001**, *105*, 1020.
 (37) Zhao, Y.; Houk, K. N.; Olson, L. P. *J. Phys. Chem. A* **2004**, *108*, 5864.
 (38) Atkinson, R.; Arey, J. *Chem. Rev.* **2003**, *103*, 4605.
 (39) Espada, C.; Grossenbacher, J.; Ford, K.; Couch, T.; Shepson, P. B. *Int. J. Chem. Kinet.* **2005**, *37*, 675.
 (40) Carter, W. P. L.; Atkinson, R. *J. Atmos. Chem.* **1985**, *3*, 377.
 (41) Day, D. A.; Dillon, M. B.; Wooldridge, P. J.; Thornton, J. A.; Rosen, R. S.; Wood, E. C.; Cohen, R. C. *J. Geophys. Res.* **2003**, *108*, 4501.
 (42) O'Brien, J. M.; Czuba, E.; Hastie, D. R.; Francisco, J. S.; Shepson, P. B. *J. Phys. Chem. A* **1998**, *102*, 8903.
 (43) Lesar, A.; Hodosscek, M.; Drougas, E.; Kosmas, A. M. *J. Phys. Chem. A* **2006**, *110*, 7898.

[or, equivalently, the nitrate yields] could be obtained, of <0.10 for the $\text{CH}_3\text{O}_2 + \text{NO}$ reaction and <0.05 for the $\text{C}_2\text{H}_5\text{O}_2 + \text{NO}$ reaction over the temperature and pressure ranges observed. Their results did not observe nitrate formation directly, but could provide an upper limit to its formation.

In this paper, theoretical methods are used to evaluate the molecular structures, vibrational frequencies, and the proton affinities of methyl nitrite and methyl peroxyxynitrite, as well as their protonated forms, to determine if protonated alkyl nitrates and alkyl nitrites provide a unique signature for the parent.

II. Computational Methods

Geometry optimizations for methyl nitrite and methyl peroxyxynitrite, along with various protonated forms for each were determined with Becke's three-parameter density functional (B3LYP) method,^{44,45} the quadratic configuration interaction with single and double excitations (QCISD)⁴⁶ method, and the QCISD(T) approach,⁴⁶ which incorporates a perturbational estimate of the effects of connected triple excitations. The QCISD(T) method has been shown to give very similar structural and energetic results as the CCSD(T) method. Our choice for using the QCISD(T) method is to calibrate results of systems in this study with those in the literature. These methods were used with the 6-31G(d) basis set.⁴⁶ Harmonic vibrational frequencies were determined for all structures at the B3LYP, QCISD, and QCISD(T) levels of theory using the 6-31G(d) basis set to verify whether the protonated structures were genuine minima. In order to obtain a more accurate prediction of the energies, single point energy calculations were performed with the QCISD(T) method in conjunction with three additional basis sets: the 6-311++G(2d,2p), the 6-311++G(2df,2p), and the 6-311++G(3df,3pd) basis sets. The GAUSSIAN 03 program⁴⁸ was used in all calculations (the complete ref 48 is given in the Supporting Information).

III. Results and Discussion

A. Protonation of Simple Alkyl Nitrates and Nitrites. 1. Protonated CH_3ONO . **a. Methyl Nitrite.** Several calculations have previously been done on methyl nitrite using various methods and basis sets, most not taking into account the effects of electron correlation. Veken et al.⁴⁹ used Hartree–Fock theory, employing both the 3-21G and 6-31G(d) basis sets, and focused more on the structural parameters for the optimized geometries of CH_3ONO . Baer et al.⁵⁰ used the STO-3G basis set at the 3-21G and 6-31G levels for various CH_3NO_2^+ isomers, focusing on the dissociation mechanism of methyl nitrite ions. McKee^{51,52} performed several ab initio studies, taking into account electron correlation by using the MP2 level on the CH_3NO_2 potential energy surface and focusing on rearrangement pathways on this surface.

Calculated features of the equilibrium structure for methyl nitrite (CH_3ONO) is presented in Supporting Information Table I; Figure 2 depicts its structure. There are two dihedral angles defining its conformation: the HCON and CONO dihedral

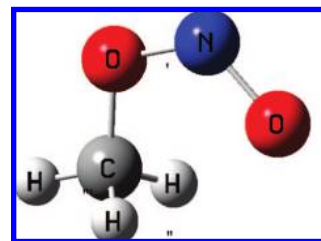


Figure 2. Lowest energy structure of the trans, cis conformer of CH_3ONO .

Table 1. Relative Energies for the Protonated Structures of CH_3ONO (kcal/mol)^a

species	conformation	B3LYP	QCISD	QCISD(T)
CH_3ONO	tc	0.0	0.0	0.0
$\text{CH}_3\text{OH}\cdot\text{NO}^+$	tct	190.8	193.1	191.8
CH_3ONOH^+	tct	175.8	174.3	173.5

^a Only the lowest energy structures for the two-protonated oxygen sites for CH_3ONO are shown here.

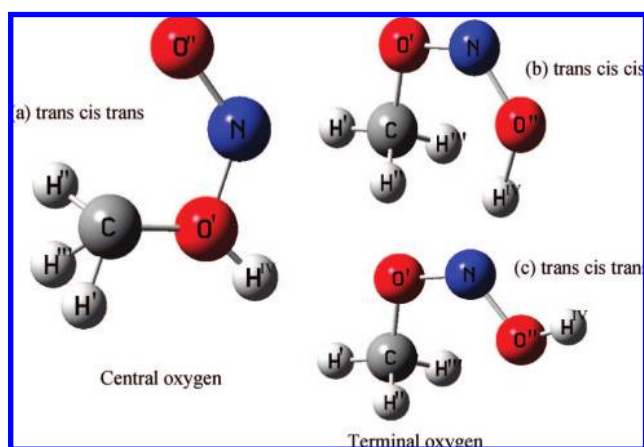


Figure 3. Different structural isomers of oxygen-protonated CH_3ONO .

angles. The minimum energy structure for CH_3ONO is a trans, cis (tc) conformation with a C_1 symmetry. Table 1 shows the close agreement between the B3LYP, QCISD, and QCISD(T) structures, in particular for the tc conformer of CH_3ONO . When we compare the QCISD and QCISD(T) structures, the largest change is 0.006 \AA in the N–O bond. Between the B3LYP and QCISD(T) structures, the change in this bond is 0.013 \AA , which shows the importance of using the QCISD(T) level of theory.

b. Protonated Methyl Nitrite: A Conformational Study. The central and terminal oxygens are the two-protonation sites for CH_3ONO , shown in Figure 3. Optimization and frequency calculations using three levels of theory (B3LYP, QCISD, QCISD(T)) were performed on four conformations of the CH_3ONO structure (tt, ct, tc, cc), 24 calculations. The tc conformer yielded the lowest energy structure and from here, both oxygen sites were protonated, with 24 optimization and frequency calculations done on two conformations, tct and tcc. There are three dihedral angles that define the protonated conformations of CH_3ONO : the HCON, CONO, and HONO (central protonated) or ONOH (terminal protonated in trans or cis mode) dihedral angles. The tct conformer yielded the lowest energy structure for both protonation sites with CH_3ONO preferring to protonate on the central oxygen in the tct conformation.

(44) Becke, A. D. *J. Chem. Phys.* **1993**, *98*, 5648.

(45) Lee, C.; Yang, W.; Parr, R. G. *Phys. Rev. B* **1988**, *37*, 785.

(46) Pople, J. A.; Head-Gordon, M.; Raghavachari, K. *J. Chem. Phys.* **1987**, *87*, 5968.

(47) Hehre, W. J.; Ditchfield, R. P.; Pople, J. A. *J. Chem. Phys.* **1972**, *56*, 2257.

(48) Frisch, M. J. et al., *Gaussian 03*; Gaussian Inc.: Wallingford, CT, 2004.

(49) van der Veken, B. J.; Maas, R.; Guirgis, G. A.; Stidham, H. D.; Sheehan, T. G.; Durig, J. R. *J. Phys. Chem.* **1990**, *94*, 4029.

(50) Baer, T.; Hass, J. R. *J. Phys. Chem.* **198690**, 451.

(51) McKee, M. L. *J. Am. Chem. Soc.* **1986**, *108*, 5784.

(52) McKee, M. L. *J. Phys. Chem.* **1986**, *90*, 2335.

Table 2. Proton Affinity for the Protonated Structure of CH₃ONO

method	basis set	proton affinity (kcal/mol)	
		CH ₃ OH·NO ⁺	CH ₃ ONOH ⁺
QCISD(T)	6-31G (d)	191.8	173.5
	6-311++G (2d, 2p)	197.9	175.3
	6-311++G (2df, 2p)	194.3	174.6
	6-311++G (3df, 3pd)	195.2	175.8

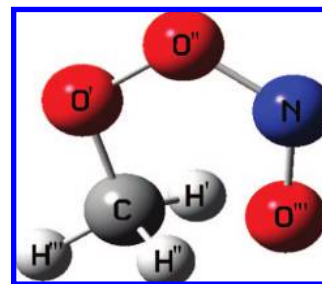
Supporting Information Table II shows the structural data for the equilibrium geometries for the conformers of the protonated CH₃ONO structure. Comparing the QCISD(T) values for the unprotonated NO bond in the tc CH₃ONO structure with the protonated NO bond in the tct central oxygen protonated CH₃ONO structure, we find a large structural change of 0.56 Å. The changes in the HCO, CON, and ONO bond angles are between 3 and 7° after protonation. For the HCON and CONO dihedral angles, the change is 20° and 32°, respectively.

Relative energies for the protonated structures of CH₃ONO are given in Table 1 (with the total and relative energies given in Supporting Information Table III). The main result from the relative energies is to ascertain the lowest energy isomer of protonated methyl nitrite. Note that the tcc structure is not shown in this table because the values for the central oxygen protonation for the two conformations are chemically equivalent. Methyl nitrite prefers to protonate on the central oxygen in the tct conformation, with an 18.3 kcal/mol difference between the central and terminal protonated oxygen sites in that same conformation. The difference between the relative energies of the protonated terminal oxygen is 13 kcal/mol, relatively close in terms of energies. If we compare the methods, then there is 1 kcal/mol difference between the B3LYP and QCISD(T) for the tct central oxygen protonated structure with a 2.3 kcal/mol difference between B3LYP and QCISD methods and a 1.3 kcal/mol difference between QCISD and QCISD(T) methods. For the terminal oxygen protonation, in tct, we find a difference of 2 kcal/mol between the B3LYP and QCISD(T), a 1.5 kcal/mol between B3LYP and QCISD, and a 0.8 kcal/mol between QCISD and QCISD(T).

Protonation on the central oxygen of the tc CH₃ONO structure yields a complex between CH₃OH and NO⁺. If we were to compare this result with the literature⁵³ for HONO, then the protonation of HONO yields a complex between H₂O and NO⁺. Our finding of a CH₃OH·NO⁺ complex for CH₃ONO is consistent with the literature observations for HONO, as both protonate on the central oxygen, yielding an NO⁺.

c. Proton Affinity of Methyl Nitrite. Geometry optimizations were performed on the two lowest energy protonated structures of methyl nitrite, CH₃OH⁺NO (central oxygen in the tct conformation) and CH₃ONOH⁺ (terminal oxygen in the tct conformation), in order to best estimate and compare proton affinity energetics. Table 2 shows the proton affinity for the two protonated structures of methyl nitrite with the QCISD(T) method and its basis sets, from 6-31G(d) to the enlarged 6-311++G(3df, 3pd) basis set. At the highest level of theory, the proton affinity is estimated to be 195.2 kcal/mol. If we compare this result with HONO's proton affinity, 191.5 kcal/mol,⁵⁵ we see there is consistency between the two systems. We can also see that from increasing the R-group from H to CH₃, the proton affinity increases, indicating a methyl effect.

2. Protonated CH₃OONO. a. Methyl Peroxynitrite. Several calculations have previously been done on methyl peroxynitrite

**Figure 4.** Lowest energy structure of the trans, cis, cis conformer of CH₃OONO.**Table 3.** Relative Energies for the Protonated Structures of CH₃OONO (kcal/mol)^a

species	conformation	B3LYP	QCISD	QCISD(T)
CH ₃ OONO	tcc	0.0	0.0	0.0
CH ₃ OH ⁺ ONO	tccc	172.2	171.1	172.5
CH ₃ OOH·NO ⁺	tccc	192.1	195.8	193.1
CH ₃ OONOH ⁺	tcct	174.9	171.7	170.9

^a Only the lowest energy structures for the three-protonated oxygen sites for CH₃OONO are shown here.

using various methods and basis sets. Zhao et al.³⁷ calculated geometries and energies with DFT using the (U)B3LYP functional with the 6-31+G(d) basis set for the dissociation reactions of peroxynitrous acid and methyl peroxynitrite. Recently, Lesar et al.⁴³ have used ab initio and DFT techniques in obtaining the potential energy surface of the CH₃O₂ + NO reaction. The optimizations were done with the B3LYP/6-311++G(d,p) and MP2/6-311++G(d,p) levels of theory and focused on minima and transition states. For methyl peroxynitrite, we have once again taken into account electron correlation effects by employing the QCISD and QCISD(T) methods.

Calculated features of the equilibrium structure for methyl peroxynitrite (CH₃OONO) are presented in Supporting Information Table IV; Figure 4 depicts its structure. There are three dihedral angles that define its conformation: the HCOO, COON, and OONO dihedral angles. The minimum energy structure for CH₃OONO is a tcc conformation with a C₁ symmetry. Table 5 shows the close agreement between the B3LYP, QCISD, and QCISD(T) structures, in particular for the tcc conformer of CH₃OONO. When we compare the QCISD and QCISD(T) structures, the largest change is 0.030 Å in the O–N bond. Between the B3LYP and QCISD(T) structures, the change in this bond is 0.044 Å.

b. Protonated Methyl Peroxynitrite: A Conformational Study. The first central, second central, and terminal oxygen are the three-protonation sites on CH₃OONO, shown in Figure 5. Optimization and frequency calculations, using three levels of theory (B3LYP, QCISD, QCISD(T)), were performed on eight conformations of the CH₃OONO structure (tct, ttt, ttc, tcc, ctc, ctt, cct, ccc), 48 calculations. There are four dihedral angles that define the protonated conformations of CH₃OONO: the HCOO, COON, OONO, and HOON (1st central oxygen protonation), HONO (2nd central oxygen protonation), or ONOH (terminal oxygen in trans or cis mode) dihedral angles. The tcc conformer yielded the lowest energy structure, and from here, the three oxygen sites were protonated, with 54 optimization and frequency calculations performed on two conformations, tccc and tcct. The tccc conformer yielded the lowest energy structure for the first two-protonation sites and a tcct conformer for the terminal site. However, CH₃OONO prefers

(53) Francisco, J. S. *J. Chem. Phys.* **2001**, *115*, 2117.

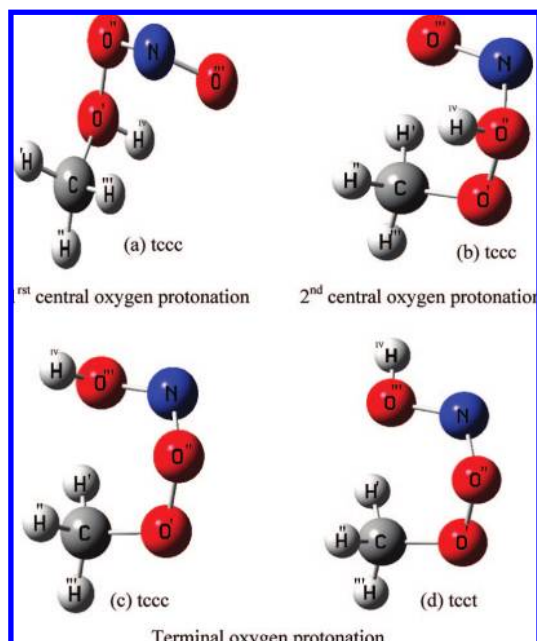


Figure 5. Different structural isomers of oxygen-protonated CH_3OONO .

Table 4. Proton Affinity for the Protonated Structure of CH_3OONO

method	basis set	proton affinity (kcal/mol)		
		$\text{CH}_3\text{OH}^+\text{ONO}$	$\text{CH}_3\text{OOH}\cdot\text{NO}^+$	$\text{CH}_3\text{OONOH}^+$
QCISD(T)	6-31G (d)	172.5	193.1	170.9
	6-311++G (2d, 2p)	175.6	198.1	172.8
	6-311++G (2df, 2p)	173.4	194.4	172.4
	6-311++G (3df, 3pd)	174.5	195.8	173.4

to protonate on the second central oxygen in the tccc conformation.

Supporting Information Table V shows the structural data for the equilibrium geometries for the conformers of the protonated CH_3OONO structure. When comparing the QCISD(T) for the unprotonated O–N bond in the tcc CH_3OONO structure with the protonated O–N bond in the tccc second central oxygen protonated CH_3OONO structure, we find a large structural change of 0.643 Å. The changes in the OON and ONO bond angles are 17° and 15°, respectively after protonation. For the COON and OONO dihedral angles, the change is 28° and 9°, respectively.

Relative energies for the protonated structures of CH_3OONO are given in Table 3, (with the total and relative energies given in Supporting Information Table VI). Note that the tcct structures for the first and second central protonated methyl peroxy nitrite are not shown here as their values for the two conformations are chemically equivalent. Methyl peroxy nitrite prefers to protonate on the second central oxygen in the tccc conformation, with a 21 kcal/mol difference between the first and second central protonated oxygen sites (both in the tccc conformations) and a 22 kcal/mol difference between the second central and terminal protonated oxygen sites (in the tccc and tcct conformations, respectively). The difference between the relative energies of the protonated terminal oxygen is 9.5 kcal/mol; relatively close in terms of energies. If we compare the methods, there is a 0.3 kcal/mol difference and a 1 kcal/mol difference between the B3LYP and QCISD(T) methods for the tccc first central and second central oxygen protonated structures respectively. Between B3LYP and QCISD, there is a 0.5 kcal/mol difference

Table 5. Protonation Pattern for Alkyl Nitrates and Alkyl Nitrites

species	preferred protonation pattern	proton affinity (kcal/mol)
HOONO	$\text{HOOH}\cdot\text{NO}^+$	182.1
HONO_2	$\text{H}_2\text{O}\cdot\text{NO}_2^+$	182.5
CH_3OONO	$\text{CH}_3\text{OOH}\cdot\text{NO}^+$	195.8
CH_3ONO_2	$\text{CH}_3\text{OH}\cdot\text{NO}_2^+$	176.9

for the first central oxygen and a 3.7 kcal/mol difference for the second central oxygen. Between QCISD and QCISD(T) methods, there is a 0.8 kcal/mol difference for the first central oxygen and a 2.7 kcal/mol difference for the second central oxygen. For the terminal oxygen protonation, tcct, we find a difference of 4 kcal/mol between the B3LYP and QCISD(T) methods, a 3.2 kcal/mol between B3LYP and QCISD methods and a 0.8 kcal/mol between QCISD and QCISD(T) methods.

Protonation on the second central oxygen of the tccc CH_3OONO structure yields a complex between CH_3OOH and NO^+ . For comparison, protonation of CH_3OONO with HOONO ,⁵⁴ yields a complex between HOOH and NO^+ . Both CH_3OONO with HOONO protonate on the second central oxygen yielding an NO^+ . If we compare CH_3OONO with CH_3ONO_2 ,⁵⁵ we find that protonation of CH_3ONO_2 yields a complex between CH_3OH and NO_2^+ . Here, the protonation sites differ, (2nd central oxygen for CH_3OONO as opposed to first central oxygen for CH_3ONO_2) and the yields differ, (NO^+ as opposed to NO_2^+).

c. Proton Affinity of Methyl Peroxynitrite. Geometry optimizations were performed on the three lowest energy protonated structures of methyl peroxy nitrite, $\text{CH}_3\text{OH}^+\text{NO}_2$ (1st central oxygen site at the tccc conformation), $\text{CH}_3\text{OOH}^+\text{NO}$ (2nd central oxygen site at the tccc conformation), and $\text{CH}_3\text{OONOH}^+$ (terminal oxygen site at the tcct conformation), in order to best estimate and compare the geometries and proton affinity energetics. Table 4 shows the proton affinity for the three protonated structures of methyl peroxy nitrite with the QCISD(T) method and its basis sets that run from 6-31G(d) to the enlarged 6-311++G(3df,3pd) basis set. At the highest level of theory, the proton affinity is estimated to be 195.8 kcal/mol. If we compare the proton affinity for CH_3OONO (195.8 kcal/mol) and HOONO (182.1 kcal/mol),⁵⁶ we see that the proton affinity increases with increasing the R-group, from H to CH_3 . The 13.7 kcal/mol difference indicates a methyl effect. Comparing the nitrites going from CH_3ONO to CH_3OONO , we find an increase in the proton affinities.

B. Comparison of Protonated CH_3OONO and CH_3ONO_2 . When comparing the ab initio results for protonated methyl peroxy nitrite (CH_3OONO) and methyl nitrate (CH_3ONO_2),⁵⁵ we find that the lowest energy forms for CH_3OONO is a complex between CH_3OOH and NO^+ , for protonation on the second central oxygen. The lowest energy form for CH_3ONO_2 is a complex between CH_3OH and NO_2^+ , for protonation on the first central oxygen. Table 5 shows the protonation patterns for these alkyl nitrites and alkyl nitrates with their respective proton affinities. It also shows the protonation patterns for peroxy nitrous acid (HOONO)⁵⁶ and nitric acid (HONO_2).⁵⁵ For HOONO and CH_3OONO , proton affinities are 182.1 and 195.8 kcal/mol, respectively. Both of these structures yield an NO^+ upon

(54) Santiano, R.L...; Francisco, J. S. *J. Chem. Phys.* **2004**, *121*, 9498.

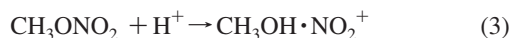
(55) Lee, T. J.; Rice, J. E. *J. Am. Chem. Soc.* **1992**, *114*, 8247.

(56) Chong, S. L.; Myers, R. A.; Franklin, J. L. *J. Chem. Phys.* **1972**, *56*, 2427.

protonation on the second central oxygen, and we can see how as the size of the R group increases, the proton affinity increases. For CH_3ONO_2 and HONO_2 , their proton affinities are 176.9 and 182.5 kcal/mol, respectively. Both species yield an NO_2^+ upon protonation on the first central oxygen.

There is a general protonation trend for alkyl nitrites and alkyl nitrates. For the nitrites, increasing the R-group from H to CH_3 , increases the proton affinity, (going from HONO to CH_3ONO and from HOONO to CH_3OONO). The proton affinity also increases when going from CH_3ONO to CH_3OONO . Also note that going from HONO to HOONO, the proton affinity decreases. For the nitrates, increasing the R-group from H to CH_3 , decreases the proton affinity, (going from HONO_2 to CH_3ONO_2). There are other trends to note. For HOONO, the proton affinity is slightly lower than HONO_2 by 0.4 kcal/mol. For CH_3OONO (protonation on the first central oxygen), the proton affinity is again slightly lower than CH_3ONO_2 by 2.4 kcal/mol. In comparing nitrates with nitrites, the data suggest that proton affinity values for RONO_2 ($\text{CH}_3\text{ONO}_2 + \text{H}^+ \rightarrow \text{CH}_3\text{OH} \cdot \text{NO}_2^+$, 176.9 kcal/mol) are lower than RONO ($\text{CH}_3\text{ONO} + \text{H}^+ \rightarrow \text{CH}_3\text{OH} \cdot \text{NO}^+$, 195.2 kcal/mol). This is supported by comparison of HONO_2 (182.5 kcal/mol) with HONO (191.5 kcal/mol).⁵³ There is also consistency for the proton affinity for the nitrite series (CH_3OONO , CH_3ONO , and HONO). The proton affinity values are comparable (195.8, 195.2, and 191.5 kcal/mol, respectively).

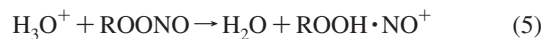
C. Implications for the Protonation Trends. In order to determine what fraction of $\text{RO}_2 + \text{NO}$ and $\text{RO} + \text{NO}_2$ gives alkyl nitrates and alkyl nitrites, the present work suggests that hydrogen protonation of CH_3OONO and CH_3ONO_2 yields a unique product distribution associated with each isomer:



The protonated forms for methyl peroxynitrite and methyl nitrate lead to different complexes ($\text{ROOH} + \text{NO}^+$ and $\text{ROH} + \text{NO}_2^+$) that can be identified, at least for the lowest energy forms of these protonated species. Ab initio calculations predict that protonation provides an effective method for measuring the $\text{CH}_3\text{OONO}/\text{CH}_3\text{ONO}_2$ branching ratio from the reactions of $\text{CH}_3\text{O}_2 + \text{NO}$ and $\text{CH}_3\text{O} + \text{NO}_2$, since the proton affinity of CH_3OONO (195.8 kcal/mol) is 18.9 kcal/mol greater than the proton affinity of CH_3ONO_2 (176.9 kcal/mol). Protonation is predicted to be poor for resolving the HOONO/HONO₂ branching ratio, since the proton affinity of HOONO (182.1 kcal/mol)

is similar to the proton affinity of HONO_2 (182.5 kcal/mol), within computational uncertainties.

From this, we propose proton transfer mass spectrometry experiments as opposed to direct optical spectroscopic approaches, which have their limitations, to cleanly and unambiguously measure the branching ratios of these species. Because protonation of methyl peroxynitrite and methyl nitrate and their respective isomers result in different and distinct product speciation, direct protonation can be a useful method for alkyl nitrite/nitrate detection. There are several approaches to experimentally protonate these species. One common technique is proton transfer by H_3O^+ , through the proton transfer reaction:



For $\text{R} = \text{CH}_3$, it is exothermic by 27.8 kcal/mol, as determined by a comparison of the proton affinity of water (168 kcal/mol)⁵⁶ and that of CH_3OONO (195.8 kcal/mol). These findings support the essential conclusion presented above, and indeed suggest that proton transfer could be a useful method for nitrite/nitrate branching ratio determination.

IV. Conclusions

All possible protonated sites and conformations have been examined for methyl nitrite and methyl peroxynitrite, via ab initio and density functional methods. We find that for methyl nitrite, the preferred site of protonation is on the central oxygen, resulting in a complex of CH_3OH and NO^+ . At the QCISD(T)/6-311++G(3df,3pd) level of theory, the best estimate of the proton affinity is 195.2 kcal/mol. For methyl peroxynitrite, the preferred site of protonation is on the second central oxygen, resulting in a complex of CH_3OOH and NO^+ . At the QCISD(T)/6-311++G(3df,3pd) level of theory, the best estimate of the proton affinity is 195.8 kcal/mol. The results suggest a general protonation trend for alkyl nitrites and alkyl nitrates, which suggests a new approach in determining the branching ratios from a protonation experiment.

Supporting Information Available: Structural data for methyl nitrite and protonated methyl nitrite (Tables I and II); total and relative energies for protonated structures of methyl nitrite (Table III); structural data for methyl peroxynitrite data (Table IV) and protonated data (Table V); total and relative energies for protonated methyl peroxynitrite (Table VI); complete ref 48. This material is available free of charge via the Internet at <http://pubs.acs.org>.

JA8045662